AGU PUBLICATIONS

Journal of Advances in Modeling Earth Systems

RESEARCH ARTICLE

10.1002/2016MS000635

Key Points:
- The climate models examined do not reproduce the observed sensitivity of TC intensity to SST
- The climate models realistically simulate the thermodynamic conditions needed for intense TCs
- The most intense simulated TCs do not occur over areas with optimal thermodynamic conditions

Correspondence to:
S. E. Strazzo,
s.e.strazz@gmail.com

Citation:
Strazzo, S. E., J. B. Elsner, T. E. LaRow, H. Murakami, M. Wehner, and M. Zhao (2016), The influence of model resolution on the simulated sensitivity of North Atlantic tropical cyclone maximum intensity to sea surface temperature, *J. Adv. Model. Earth Syst.*, *8*, 1037–1054, doi:10.1002/2016MS000635.

Received 25 JAN 2016
Accepted 22 MAY 2016
Accepted article online 27 MAY 2016
Published online 10 JUL 2016

The influence of model resolution on the simulated sensitivity of North Atlantic tropical cyclone maximum intensity to sea surface temperature

S. E. Strazzo[1,2], J. B. Elsner[1], T. E. LaRow[3], H. Murakami[4,6], M. Wehner[5], and M. Zhao[4]

[1]Department of Geography, Florida State University, Tallahassee, Florida, USA, [2]Department of Geography and Environmental Engineering, United States Military Academy, West Point, New York, USA, [3]Verato, Inc., McLean, Virginia, USA, [4]NOAA Geophysical Fluid Dynamics Laboratory, Princeton, New Jersey, USA, [5]Lawrence Berkely National Laboratory, Berkely, California, USA, [6]Meteorological Research Institute, Tsukuba, Ibaraki, Japan

Abstract Global climate models (GCMs) are routinely relied upon to study the possible impacts of climate change on a wide range of meteorological phenomena, including tropical cyclones (TCs). Previous studies addressed whether GCMs are capable of reproducing observed TC frequency and intensity distributions. This research builds upon earlier studies by examining how well GCMs capture the physically relevant relationship between TC intensity and SST. Specifically, the influence of model resolution on the ability of a GCM to reproduce the sensitivity of simulated TC intensity to SST is examined for the MRI-AGCM (20 km), the GFDL-HiRAM (50 km), the FSU-COAPS (0.94°) model, and two versions of the CAM5 (1° and 0.25°). Results indicate that while a 1°C increase in SST corresponds to a 5.5–7.0 m s^{-1} increase in observed maximum intensity, the same 1°C increase in SST is not associated with a statistically significant increase in simulated TC maximum intensity for any of the models examined. However, it also is shown that the GCMs all capably reproduce the observed sensitivity of potential intensity to SST. The models generate the thermodynamic environment suitable for the development of strong TCs over the correct portions of the North Atlantic basin, but strong simulated TCs do not develop over these areas, even for models that permit Category 5 TCs. This result supports the notion that direct simulation of TC eyewall convection is necessary to accurately represent TC intensity and intensification processes in climate models, although additional explanations are also explored.

1. Introduction

Global climate models (GCMs) are now relied upon to assess the impact of climate change on a wide range of meteorological phenomena, including tropical cyclones (TCs) [e.g., *Knutson et al*., 2010; *Christensen et al*., 2013]. Although insufficient resolution prevents GCMs from resolving TC inner core convection and maximum wind speeds, recent research using models with horizontal grid spacing ranging from 10 to 100 km demonstrates that many GCMs are able to reproduce the overall frequency and interannual variability of TC activity over the North Atlantic basin [e.g., *Yoshimura and Sugi*, 2005; *LaRow et al*., 2008; *Zhao et al*., 2009; *Kim et al*., 2014; *Wehner et al*., 2014; *Zarzycki and Jablonowski*, 2014]. For example, results from *LaRow et al*. [2008] demonstrate that a GCM with a T126 horizontal resolution (~0.94°) reasonably simulates the effect of the El Niño/Southern Oscillation on North Atlantic TC frequency beginning in 1995. Furthermore, recent higher-resolution modeling studies by *Wehner et al*. [2015] and *Zarzycki and Jablonowski* [2014] successfully generate TCs with wind speed distributions that better match observations. These results suggest that as resolution continues to improve, climate models may be able to better predict not only future changes in TC frequency, but also intensity.

The research presented here examines the influence of model resolution on the ability of climate models to simulate the physically relevant statistical relationship between maximum TC intensity and sea surface temperature (SST). Prior studies have tested the influence of model resolution on various metrics of simulated TC activity [e.g., *Murakami and Sugi*, 2010; *Walsh et al*., 2013], however these studies do not address some aspects of the physical relationship between model-generated TCs and SST. Much of this previous research examines GCM simulations spanning several resolutions to compare TC frequency and intensity statistics

among model runs. For example, *Wehner et al*. [2015] present the effects of model resolution on the ability of the Community Atmosphere Model (CAM5) to generate intense TCs and simulate inter/intraannual variability. As expected, the 0.25° version of the CAM5 generates much stronger TCs (including some Category 5 hurricanes on the Saffir-Simpson scale) when compared to the 1° and 2° model simulations. However, *Wehner et al*. [2014] note that model representation of certain large-scale features—for example, the notorious "double ITCZ"—does not improve in the higher-resolution version of the model. It is possible that parameterization (rather than resolution) has a greater influence on some of these larger scale features. Similarly, *Strachan et al*. [2013] examine resolution effects for the Hadley Center's GCM and show that for this model, resolution strongly influences the ability of the model to capture TC intensity but does not appear to affect the frequency and spatial distribution of model-generated TCs. It should be noted that this result may be partially explained by the Hadley Center's specific model TC detection algorithm, which does not explicitly employ a wind speed threshold.

The present study compares the relationship between TC intensity and SST among four different GCMs with horizontal grid spacing ranging from 20 to greater than 100 km. We additionally examine output from two separate simulations by the same model, one run at 0.25° and the other at 1°. Although others have implemented similar model intercomparisons, these typically focus on TC frequency and intensity distributions [e.g., *Camargo et al*., 2005; *Caron et al*., 2011; *Villarini et al*., 2011; *Camargo*, 2013; *Walsh et al*., 2013; *Roberts et al*., 2015]. For example, *Walsh et al*. [2013] examine resolution dependence of TC formation in different GCMs and *Camargo* [2013] compares TC frequency, geographic extent, genesis potential indices, and potential intensity in 14 different climate models. We wish to build on this previous research by extending model intercomparisons to also examine the sensitivity of maximum TC intensity to SST. *Emanuel* [1986] used the analogy of a Carnot heat engine to show that the theoretical maximum potential intensity of a TC is at least partially dependent on the SST. Later empirical studies [e.g., *DeMaria and Kaplan*, 1994; *Elsner et al*., 2008] suggest that increasing SSTs may be associated with increasing TC intensity, particularly for very intense TCs. Therefore, the sensitivity of maximum TC intensity to SST is a particularly useful metric for model comparison because it may yield insight into how well model-generated TCs represent the physical processes that dictate TC intensity. High-resolution models (i.e., models with horizontal grid spacing near 0.25°) may be able to simulate TCs with intensity distributions that resemble what we observe, but do the strongest model-generated TCs form over the warmest SSTs, as is the case for observed TCs [*Elsner et al*., 2012b]?

Strazzo et al. [2015] demonstrate the ability of the Florida State University-Center for Ocean-Atmospheric Prediction Studies (FSU-COAPS) model (0.94°) to reproduce the relationship between the theoretically defined potential intensity and SST despite that model's inability to simulate the observed sensitivity of maximum intensity to SST. The FSU-COAPS model successfully simulates the thermodynamic environment needed to sustain intense TCs, but does not actually generate intense TCs. *Strazzo et al*. [2015] speculate that this occurs partly because model grid spacing is too coarse to resolve the inner core and thus the maximum wind speed of simulated TCs. *Strazzo et al*. [2015] also find that the sensitivity of observed maximum TC intensity to SST is not statistically different from the sensitivity of observed potential intensity to SST. If model resolution explains the inability of the FSU-COAPS model to simulate the sensitivity of TC maximum intensity to SST, we might expect that the sensitivity of simulated maximum intensity to SST will approach the sensitivity of simulated potential intensity to SST as model resolution increases. Therefore, in addition to the sensitivity of simulated maximum intensity to SST, the research presented here examines the sensitivity of potential intensity to SST.

This study utilizes the methods introduced in *Elsner et al*. [2012a, 2012b] and *Strazzo et al*. [2013b, 2015] to estimate the sensitivity of maximum TC intensity to SST for four GCMs. The method consists of subdividing the North Atlantic basin into a tessellation of equal-area hexagon regions. For each region, the upper limit of TC intensity is approximated as the maximum intensity that occurred over that region throughout the past ∼30 years, as was done in *Strazzo et al*. [2013b]. The sensitivity of maximum TC intensity to SST is then estimated by regressing the set of per region maximum TC intensities onto the set of per region average August–October SST. We quantify this sensitivity for observed TCs and for TCs generated by the CAM5, the Meteorological Research Institute of Japan's Atmospheric Global Climate Model (MRI-AGCM), the Geophysical Fluid Dynamics Laboratory-High-Resolution Atmospheric Model (GFDL-HiRAM), and the FSU-COAPS model.

Table 1. A Summary of all TC Data Sets Used in This Analysis[a]

Data Set	Source	Time Period	Total TCs	Maximum Intensity
Observations	*Landsea and Franklin* [2013]	1979–2009	372	78.7
MRI-AGCM	*Murakami et al.* [2012]	1979–2009	338	70.3
CAM5 0.25°	*Wehner et al.* [2015]	1979–2005	387	73.8
GFDL-HiRAM	*Zhao et al.* [2009]	1981–2009	418	40.8
FSU-COAPS	*LaRow et al.* [2008]	1982–2008	392	44.1
CAM5 1°	*Wehner et al.* [2015]	1979–2007	35	34.6

[a]Maximum TC intensities are given in units of m s^{-1}. Total TCs and Maximum intensity statistics refer only to the North Atlantic.

This research adds to previous studies in several respects. First, we extend the results presented in *Elsner et al*. [2013] to include two higher-resolution models (the CAM5 and MRI-AGCM) that successfully generate Category 4 and 5 TCs on the Saffir-Simpson scale. We also utilize output from two versions of the CAM5 with horizontal resolutions of 0.25° and 1°. This allows us to test whether the ability of a GCM to generate strong TCs influences the sensitivity of simulated TC intensity to SST. Similarly, we extend the results of *Strazzo et al*. [2015] to determine whether the difference between the sensitivity of potential and maximum intensity to SST decreases as model resolution improves. Finally, we address concerns about uncertainty by estimating the error associated with the spatial tessellation methodology. The remainder of this paper is organized as follows: section 2 summarizes the data and methods, section 3 compares the observed and simulated sensitivity of maximum TC intensity to SST, section 4 compares the observed and simulated sensitivity of potential intensity to SST, and section 5 provides a summary and discussion.

2. Data and Spatial Method

2.1. Observed and Simulated TC Data

As with previous studies, observed TC track data come from the National Hurricane Center's "best track" Atlantic hurricane database [*Landsea and Franklin*, 2013]. The best track data provide 6 hourly estimates of observed TC location, 1 min average wind speed at 10 m above the surface, and minimum central pressure. Because the 6 hourly data set does not provide the temporal or spatial resolution required for the statistical analysis applied here, we interpolate the data to obtain hourly estimates of observed TC location, 10 m wind speed, and forward motion. The interpolation method, which preserves location and attribute information at the 6 hourly observation points and uses splines and spherical geometry to estimate the interpolated points, is described more fully in *Elsner and Jagger* [2013]. Finally, to match the GCM simulation periods, only TCs occurring during the 1979–2009 time period are considered.

In addition to observed TC track data, we use observed SSTs from the Hadley Centre Sea Ice and Sea Surface Temperature (HadISST) data set [*Rayner et al*., 2003]. For each grid point, we calculate the mean August–October SST over the time period of interest. The observed potential intensity [*Bister and Emanuel*, 1998] is approximated using atmospheric fields from NASA's Modern Era ReAnalysis (MERRA) [*Rienecker et al*., 2011]. The MERRA data are available on a 1.25° by 1.25° grid. Although reanalysis products are not actual atmospheric observations, these data nevertheless provide approximate historical atmospheric conditions at the relatively high spatial and temporal resolutions that this analysis requires. We choose the MERRA data in place of other reanalysis products following results presented in *Vecchi et al*. [2013] and *Kossin* [2014], which demonstrate that the MERRA product does not contain spurious negative trends in upper troposphere and tropopause temperature. For comparison, simulated model fields are used to calculate potential intensity for each of the GCMs considered.

Observed TC track data are compared to TCs generated by four different GCMs. All of the models examined here are atmospheric models and are not coupled to an ocean model. Instead, each model is forced with prescribed monthly mean SSTs from the HadISST data set. Note that the monthly mean SSTs are interpolated to at least daily values within each model simulation. The model simulations were developed by the U.S. Climate Variability and Predictability program (CLIVAR) Hurricane Working Group in an effort to understand the TC response to rising SSTs and increasing carbon dioxide concentrations [*Walsh et al*., 2015]. Although each modeling group also ran their respective models using uniformly increased SSTs and doubled carbon dioxide concentrations, we focus our attention on the historical simulations, which vary in the exact duration by model (Table 1), but all fall within the 1979–2009 period. In the specific model

descriptions that follow, note that in addition to resolution, parameterization schemes and TC detection and tracking algorithm thresholds vary by model (Table 1). As with the best track data, all model data are provided at 6 hourly intervals and subsequently interpolated to hourly intervals.

The MRI-AGCM (v3.2) is maintained by the Meteorological Research Institute of Japan [*Mizuta et al*., 2012]. With 20 km (~0.18°) horizontal grid spacing and 64 vertical levels extending to 0.01 hPa, it is the highest resolution model we examine [*Murakami et al*., 2012]. The model cumulus parameterization scheme, which is based on the *Tiedtke* [1989] scheme, is described in full in *Yoshimura et al*. [2015]. The TC detection algorithm, described in full by *Murakami et al*. [2011], searches for a spatially and temporally concurrent 850 hPa relative vorticity maximum exceeding 2×10^{-4} s^{-1}, 850 hPa maximum wind speed exceeding 17 m s^{-1}, and a warm-core aloft. Additionally, each model-generated TC must persist for a minimum of 36 h. As with all of the models examined, we use simulated 10 m wind speeds for the calculation of the sensitivity of TC intensity to SST.

Output from two different simulations by the CAM5 (v5.1) are examined. One simulation uses a 0.23° by 0.31° mesh grid (referred to here as ~0.25° grid spacing), while the other simulation uses a 0.91° by 1.3°, or ~1° grid spacing [*Wehner et al*., 2014, 2015]. Both the 1° and 0.25° simulations are run with 30 vertical levels extending up to 2 hPa. For both simulations, deep convection is parameterized using the scheme described in *Zhang and McFarlane* [1995], while shallow convection is parameterized using the *Park and Bretherton* [2009] method. The algorithm used to detect and track TCs generated by the CAM5 is the same as that presented in *Knutson et al*. [2007]. The algorithm searches for a spatially and temporally concurrent 850 hPa relative vorticity maximum of 1.6×10^{-4} s^{-1}, surface pressure increase of 4 hPa from the storm center, and a warm-core aloft. TCs detected in the CAM5 must persist for at least 2 days and must have a maximum 10 m wind speed greater than 17 m s^{-1} during at least 2 days.

The GFDL-HiRAM features 32 vertical levels and 50 km (~0.45°) horizontal grid spacing, approximately twice as coarse as the 0.25° CAM5. The convective parameterization is based on that introduced in *Bretherton et al*. [2004]. As with the CAM5, the *Knutson et al*. [2007] detection and tracking algorithm is applied, although the requirement that model-detected TCs persist for 2 days is adjusted up to 3 days for the GFDL-HiRAM. Similarly, model-generated TCs must have maximum 10 m wind speeds exceeding 17 m s^{-1} during at least 3 days.

Finally, we consider the FSU-COAPS global spectral model, which is run at a resolution of T126 (~0.94°) with 27 vertical levels [*LaRow et al*., 2008]. Deep convection is parameterized using a relaxed Arakawa-Schubert scheme, described fully in *Hogan and Rosmond* [1991]. The TC detection algorithm is similar to that introduced in *Knutson et al*. [2007] but with some modified thresholds. For example, the 850 hPa vorticity threshold is changed to 4.5×10^{-5} s^{-1}. As with the CAM5, model-detected TCs must persist for a minimum of 2 days and also must have 10 m surface wind speeds exceeding 17 m s^{-1} during at least 2 days.

A comparison of the wind speed distributions of observed and model-generated TCs clearly illustrates the inability of the three relatively coarser-resolution simulations—the GFDL-HiRAM, FSU-COAPS, and CAM5 1°—to adequately simulate the observed range of TC wind speeds (Figure 1). In fact, these three models all fail to generate TCs with wind speeds exceeding 45 m s^{-1} (Table 1). Conversely, both of the higher-resolution GCMs generate some TCs with wind speeds greater than 65 m s^{-1}, although the MRI-AGCM wind speed distribution is much flatter than the observed distribution (Figure 1).

2.2. Spatial Tessellation Method

Although wind speed distributions are useful diagnostics, they do not provide any spatial information. For example, are the strongest model-generated TCs occurring over the same regions as the strongest observed TCs? One of the primary objectives of this research is to understand whether GCMs that generate TCs with intensities exceeding 60 m s^{-1} are better able to reproduce the sensitivity of maximum TC intensity to SST compared to GCMs that do not generate strong TCs. As in *Elsner et al*. [2013] and *Strazzo et al*. [2013b, 2015], we use a spatial tessellation approach to spatially bin TC and SST data for statistical analysis. We begin by tessellating the North Atlantic basin into equal-area hexagons—hereafter referred to as "regions"—and subsequently overlaying all TC track and SST data onto this set of regions. Observed TCs, model-generated TCs, and SSTs are all overlaid onto the same base tessellation. Hexagonal regions are selected in place of rectangular regions following *Elsner et al*. [2012a], who demonstrate that hexagons

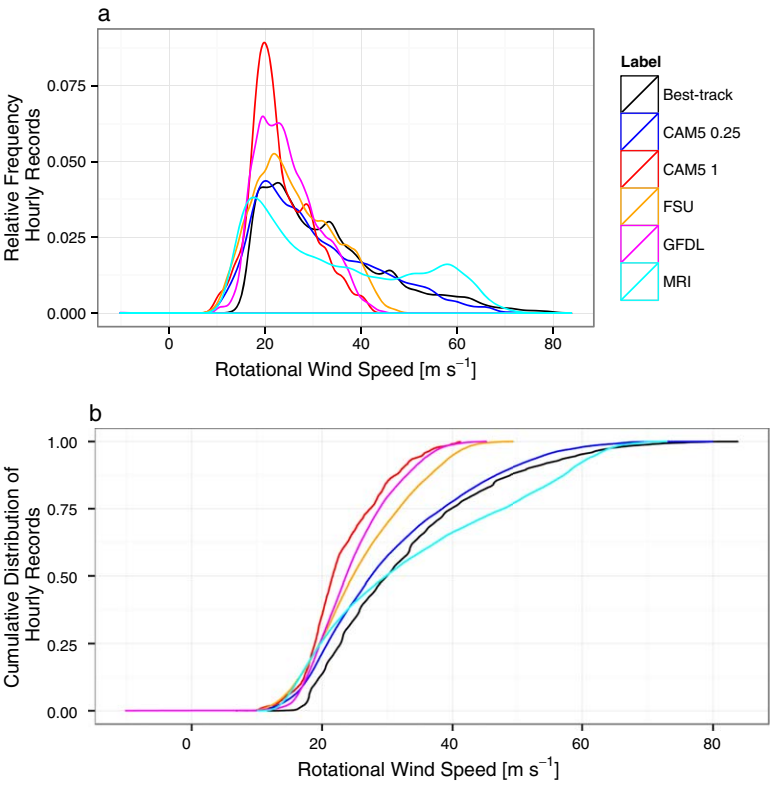

Figure 1. (a) Relative frequency distributions for observed and modeled TC wind speed and (b) cumulative distribution functions for observed and modeled TC wind speed. Wind speeds have units of m s^{-1}.

more efficiently cover TC tracks. Using this spatial tessellation method, we find the total number of observed and model-generated TCs that passed over a given region during the period(s) of interest (i.e., the per region TC count). For the analysis of each set of observed or modeled track data, we only consider those regions with a TC count of at least 15. The exception is the CAM5 1°, for which there are no regions with at least 15 TCs. We include the CAM5 1° results here but note that they cannot be directly compared to the other models. Because the spatial distribution of TCs differs among models, the specific subsets of regions used for the analysis of each set of model TC data do not necessarily match.

Previous studies examined the statistical upper limit of per region TC intensity. For example, *Elsner et al.* [2013] applied extreme value theory to the set of per region maximum TC wind speeds to estimate the statistical upper bound on regional TC intensity. However, as noted in *Strazzo et al.* [2013b, 2015], this upper limit is often underestimated for regions in the North Atlantic, likely because of insufficient TC data. Given this, the analysis presented here instead relies on the per region maximum TC intensity, which is simply the maximum intensity that occurred over each region during the time period(s) of interest. Per region maximum TC intensity is a good approximation of per region limiting TC intensity for most regions of the North Atlantic [*Strazzo et al.*, 2013b].

With the exception of the CAM5 1°, the overall number of observed TCs over the North Atlantic is generally well represented by the models (Table 1). In contrast, the spatial distributions of observed TCs (Figure 2a) and model-generated TCs (Figures 2b–2f) do not always match. Most regions over the North Atlantic experienced between 45 and 60 observed TCs during the 1979–2009 time period, with a maximum in TC activity occurring for a region off the mid-Atlantic coast of the U.S. (79 TCs). Importantly, between 45 and 60 TCs also tracked through regions in the western Caribbean and Gulf of Mexico. However, the CAM5 0.25° is the only model that simulates close to the observed number of TCs over the Gulf of Mexico during the model period of 1979–2005 (Figure 2c). Although the CAM5 0.25° performs better over the Gulf of Mexico relative to the other models, it has much higher than observed per region TC counts (>100) for regions in the far eastern portion of the basin. In fact, both the MRI-AGCM (Figure 2b) and CAM5 0.25° appear to generate a

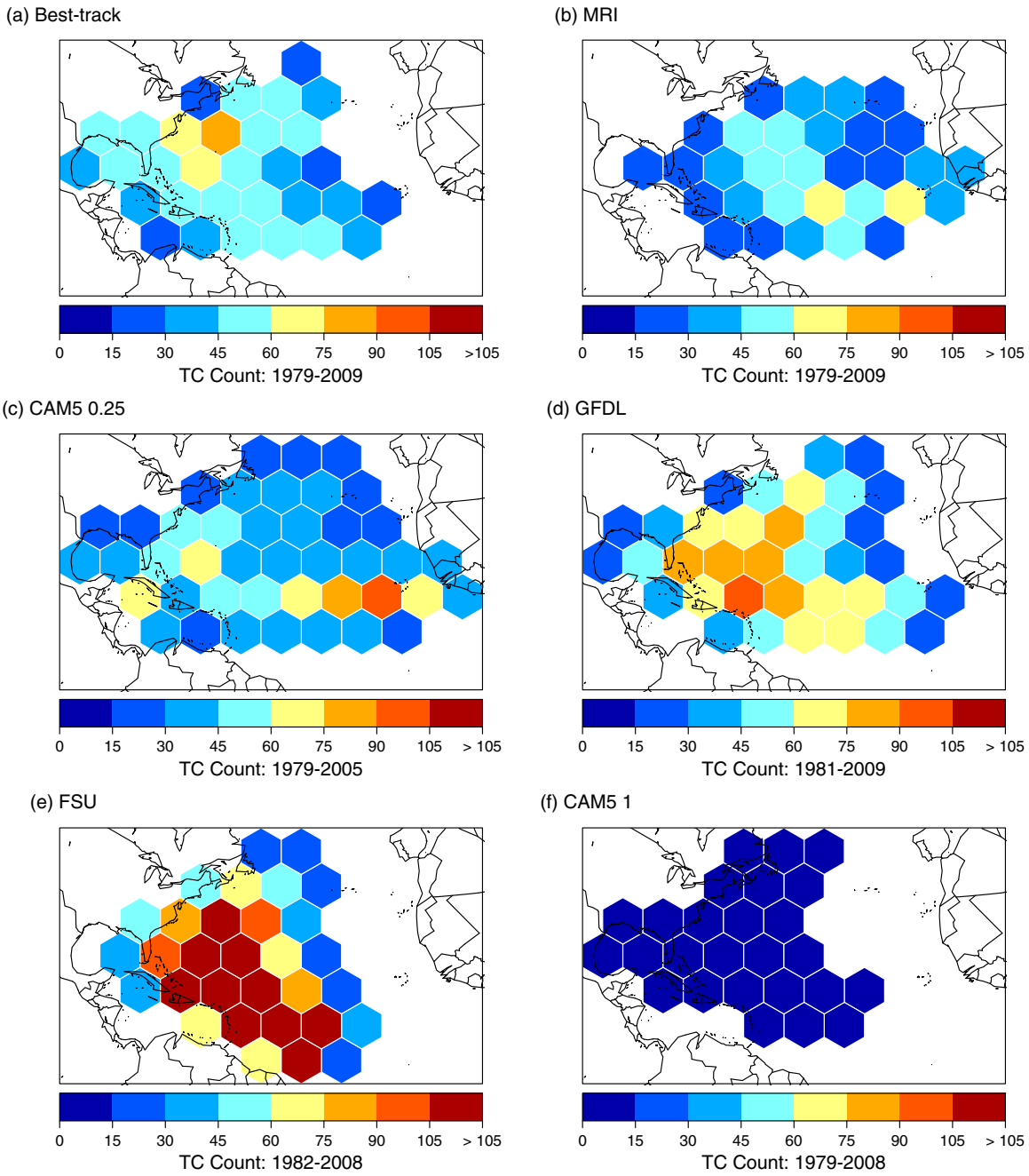

Figure 2. Per region TC counts for (Best-track; a) observed TCs and for TCs generated by the (MRI; b) MRI-AGCM, (CAM5 0.25; c) CAM5 0.25°, (GFDL; d) GFDL-HiRAM, (FSU; e) FSU-COAPS, and (CAM5 1; f) CAM5 1° models. Each plot only includes regions with a TC count of at least 15 for the respective data set, except for the CAM5 1, which did not generate a sufficient number of TCs to apply this rule.

large number of TCs immediately west of the African coast, whereas the observed spatial distribution is shifted farther west near the Cape Verde Islands. This apparent cyclogenesis bias may be an artifact of TC detection algorithms that possibly detect and begin tracking simulated TCs earlier than is done by forecasters for observed TCs. However, CAM5 0.25° TCs that form in this region also tend to recurve earlier than observed TCs, suggesting that the cyclogenesis bias exists [*Wehner et al.*, 2014]. In addition to these discrepancies, the FSU-COAPS model (Figure 2e) generates nearly all of its TC activity much farther south and east in the basin than is observed, while the CAM5 1° generates far fewer TCs than are observed. The CAM5 1° only generates 35 total TCs during the 1979–2007 simulation period, the fewest of any model considered (Table 1).

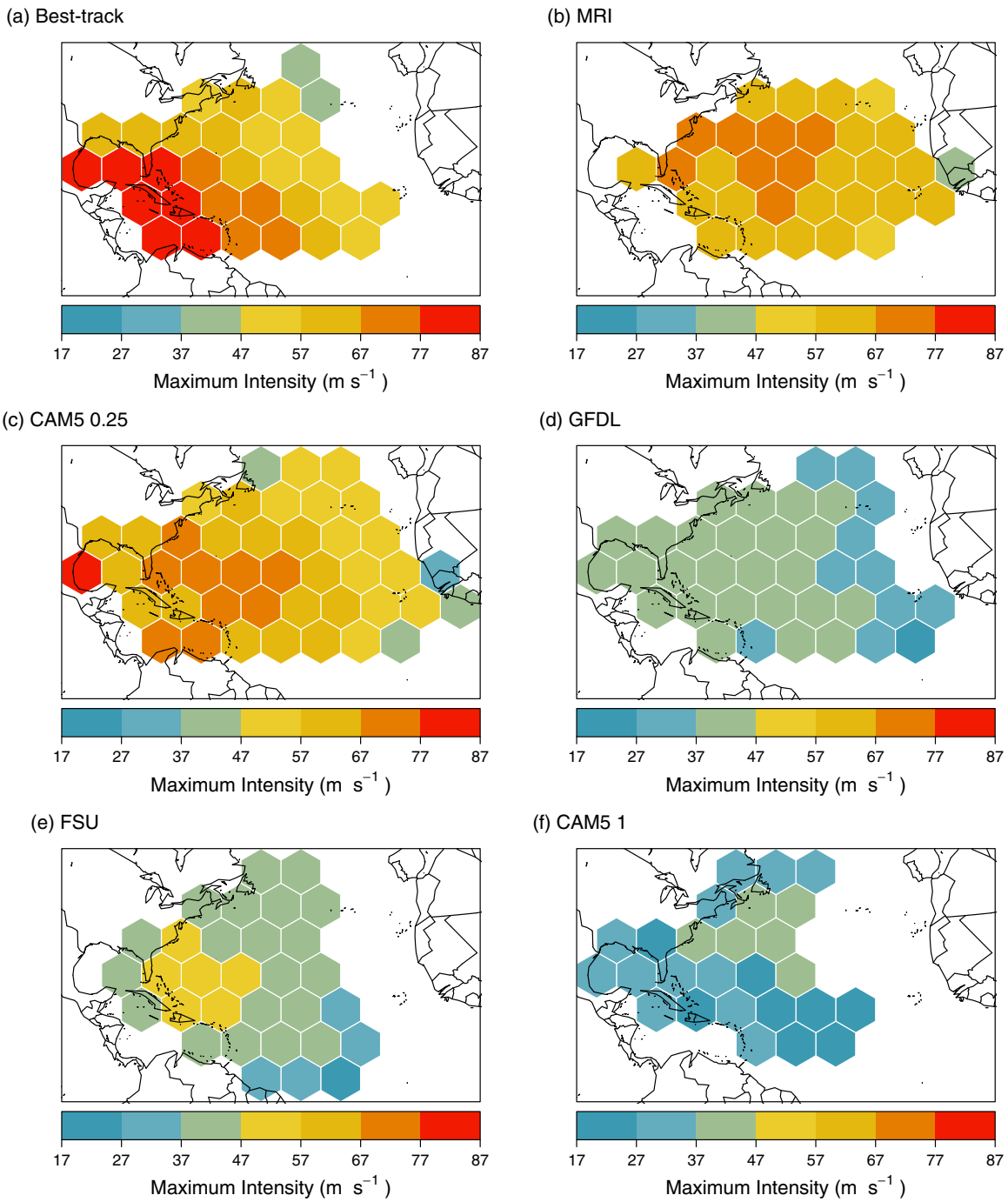

Figure 3. Per region maximum intensity (m s^{-1}) for (Best-track; a) observed TCs and for TCs generated by the (MRI; b) MRI-AGCM, (CAM5 0.25; c) CAM5 0.25°, (GFDL; d) GFDL-HiRAM, (FSU; e) FSU-COAPS, and (CAM5 1; f) CAM5 1° models. Each plot only includes regions with a TC count of at least 15 for the respective data set, except for the CAM5 1, which did not generate a sufficient number of TCs to apply this rule.

Similarly, the spatial patterns of observed and simulated maximum TC intensity do not match. Observed per region maximum intensity increases from east to west and from north to south, with the most intense TCs occurring over the western Caribbean and Gulf of Mexico (Figure 3a). Once again, the CAM5 0.25° is the only model for which the strongest TCs also occur over the Gulf of Mexico, although this is only true for the westernmost region (Figure 3c). Overall, regions with the most intense simulated TCs occur farther east in the basin than is observed. However, regions with the weakest model-generated TCs *are* located farther north in the basin for all models, which matches the observed pattern.

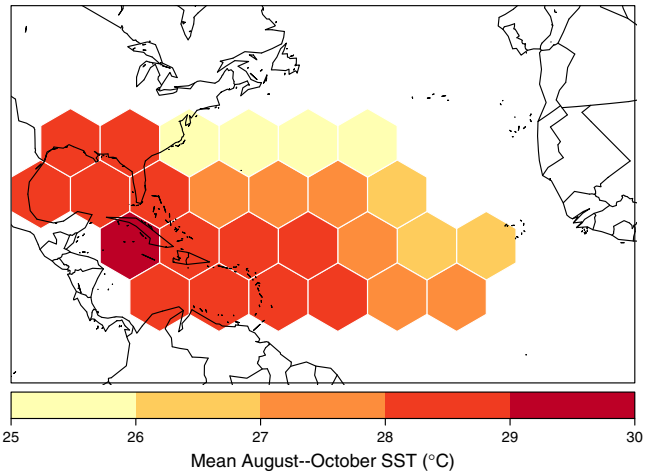

Figure 4. Per region observed mean August–October SST. Only regions with an observed TC count of at least 15 and with mean August–October SSTs $\geq$ 25°C are shown. The SST data were averaged over the 1979–2009 time period, which matches the period covered by the historical run of the MRI-AGCM.

Because we will be examining the relationship between per region maximum intensity and SST, we also map the observed spatial pattern of mean August–October SST over the 1979–2009 period (Figure 4). As with observed TC intensity, the overall pattern shows increasing SSTs from east to west and from north to south.

3. The Sensitivity of TC Maximum Intensity to SST

3.1. An Intermodel Comparison

We estimate the sensitivity of per region maximum TC intensity to SST by regressing the set of per region observed or modeled maximum TC intensities onto the set of per region mean August–October SST (Figure 5). The slope coefficients from these regressions represent the sensitivity of observed or modeled maximum TC intensity to SST (Table 2). Although per region maximum intensity is spatially autocorrelated, *Strazzo et al.* [2013b] used a spatial regression model to show that this autocorrelation does not significantly affect the sensitivity of maximum intensity to SST for the North Atlantic basin. Also note that to filter out simulated extratropical cyclones, all sensitivity values are calculated using only those regions with mean August–October SSTs of at least 25°C (as in Figure 4). This 25°C threshold is chosen because it effectively filters out the northernmost regions while also retaining enough regions to implement a meaningful statistical analysis. As reported previously by *Elsner et al.* [2013], neither the FSU-COAPS nor the GFDL-HiRAM captures the observed sensitivity of maximum TC intensity to SST. It is evident from Figures 5c and 5d that neither model generates strong TCs, and more importantly, the strongest model-generated TCs do not necessarily occur over the warmest water. Although the range of per region maximum intensities from these two models is much smaller than the observed range, our current understanding of TCs suggests that a statistically

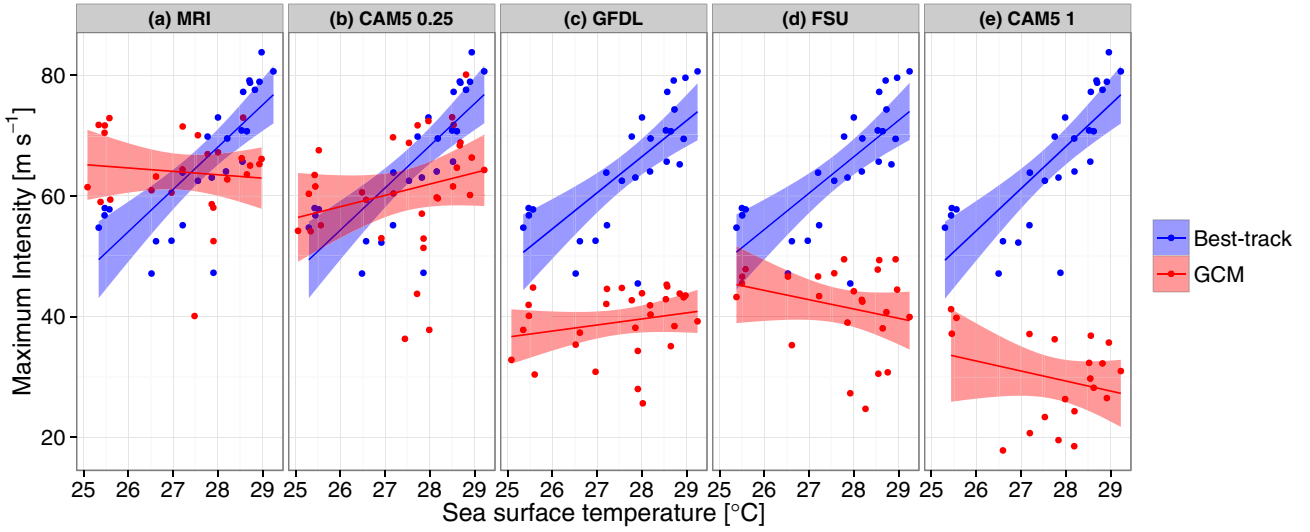

Figure 5. Regressions of regional maximum intensity onto regional mean August–October SST for TCs generated by the (a) MRI-AGCM, (b) CAM5 0.25°, (c) GFDL-HiRAM, (d) FSU-COAPS, and (e) CAM5 1° models. The sensitivities of model-generated maximum TC intensity to SST are given by the slope of the red lines. The blue lines represent the observed sensitivity of maximum TC intensity to SST for observed TCs occurring during the model period for each respective model. The shading represents the 95% confidence interval about the regression. Maximum TC intensity is given in units of m s^{-1} and SST is shown in units of °C. Only those regions with mean August–October SST $\geq$ 25°C are used in the regression.

Table 2. Summaries of Regressions of Per Region Maximum TC Intensity onto Average August–October SST for Observed and Model-Generated TCs[a]

Data Set	Sensitivity (GCM)	95% C.I. (GCM)	Sensitivity (Obs)	95% C.I. (Obs)
MRI-AGCM	−0.56	(−2.91, 1.78)	7.0	(4.58, 9.43)
CAM5 0.25°	1.9	(−0.855, 5.60)	7.0	(4.57, 9.41)
GFDL-HiRAM	1.0	(−0.659, 2.67)	6.0	(3.58, 8.39)
FSU-COAPS	−1.5	(−4.01, 0.922)	5.5	(3.61, 8.45)
CAM5 1°	−1.7	(−4.63, 1.31)	7.0	(4.56, 9.40)

[a]The second column provides the sensitivity of model-generated TCs to SST (GCM) and the third column provides the 95% confidence interval (C.I.) on this estimate. For each model time period, we also calculate the sensitivity using observed TCs. Sensitivity estimates have units of m s^{-1}/°C warming. The fourth and fifth columns provide the sensitivity and confidence interval for observed TCs over the time period matching the historical run of the model indicated in the first column. Additionally, only those regions with mean August–October SST $\geq$ 25°C are used in the regressions.

significant sensitivity to SST should exist for these model-generated TCs [*Emanuel*, 1986; *DeMaria and Kaplan*, 1994; *Elsner et al*., 2008, 2012b].

We now ask whether this discrepancy in observed versus modeled sensitivity can be remedied by employing higher-resolution models. When we observe the regressions of maximum TC intensity onto SST for TCs generated by the MRI-AGCM (Figure 5a) and the CAM5 0.25° (Figure 5b), we find conflicting results. The sensitivity of CAM5 0.25° TCs to SST is 1.9 ± 1.34 (standard error; s.e.) m $s^{-1}°C^{-1}$, although the sensitivity (slope) is not significant at the 95% confidence level (Table 2). Of the models examined here, the CAM5 0.25° best captures the observed sensitivity, especially when compared to the lower-resolution version of the CAM5. Interestingly, the highest resolution model included in this study, the MRI-AGCM, does not capture the sensitivity of maximum intensity to SST. Despite generating TCs with intensities exceeding 65 m s^{-1}, MRI-AGCM TC intensity is not sensitive to SST. It should be noted that the MRI-AGCM does not generate or track very many TCs over the Gulf of Mexico. Perhaps strong model-generated TCs do not form over this portion of the basin because GCM-generated TCs are not governed by potential intensity theory, although research presented in *Strazzo et al*. [2015] suggests that model errors associated with larger scale atmospheric features (e.g., the strength and position of the Bermuda High) may also explain the missing simulated Gulf of Mexico TCs.

It is possible that the MRI-AGCM fails to reproduce the observed sensitivity of TC maximum intensity to SST because it fails to generate or track TCs over the Gulf of Mexico—the warmest part of the basin. The track details of observed TCs may partially explain the very high observed sensitivity. Observed TCs that form over the central and eastern portions of the basin intensify as they track westward and often reach the Gulf of Mexico in an already mature state (although rapid intensification of TCs that develop over the Gulf of Mexico also occurs). To test the hypothesis that the lack of MRI-AGCM TC activity over the Gulf of Mexico explains the low-simulated sensitivity value, we reexamine the spatial pattern of observed maximum TC intensity after removing all regions over the Gulf of Mexico that do not contain MRI-AGCM TCs (Figure 6). When we recalculate the sensitivity of observed maximum TC intensity to SST using only those regions shown in Figure 6a, we find that the sensitivity value decreases from 7.0 m $s^{-1}°C^{-1}$ (all regions) to 6.7 m $s^{-1}°C^{-1}$ (Gulf of Mexico omitted). However, with standard errors of 1.18 and 1.39, respectively, this decrease in sensitivity is not statistically significant (Figure 7). In fact, even if we exclude the Gulf of Mexico *and* the western Caribbean entirely, the observed sensitivity only decreases minimally and remains statistically significant at the 95% confidence level (5.1 ± 1.55 m $s^{-1}°C^{-1}$). This suggests that the sensitivity of observed TC intensity to SST is not highly dependent on the track details. Therefore, while model errors associated with the steering flow may prevent simulated TCs from tracking over the Gulf of Mexico, this lack of simulated Gulf of Mexico activity does not necessarily explain the inability of GCMs to capture the observed sensitivity of maximum intensity to SST. Additionally, the few model-generated TCs that do occur over this region do not reach sufficiently high intensities. The reason for this may be thermodynamic (e.g., simulated TCs are not governed by the same physics as observed TCs), or dynamic (e.g., the model generates higher vertical wind shear over this region than is observed).

Strazzo et al. [2013a] note that although the GFDL-HiRAM fails to generate TCs with maximum wind speeds exceeding 45 m s^{-1}, the simulated minimum sea level pressure distribution better matches observations. Given this, we also calculate the sensitivity of minimum sea level pressure to SST. We find that as with maximum wind speed, the sensitivity of minimum sea level pressure to SST is highly significant for observed TCs (-14 ± 2.51 hPa $°C^{-1}$), but not significant for the models (Table 3). Table 3 provides sensitivity estimates at the 95% confidence level. Overall the GCMs do not reproduce the observed sensitivity of TC intensity to SST

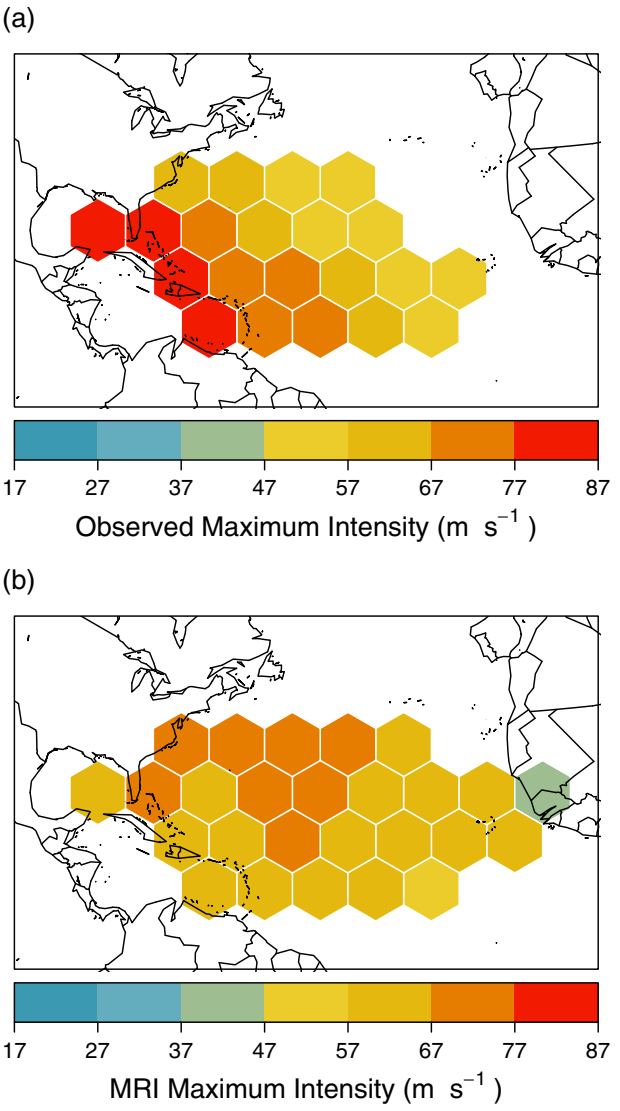

Figure 6. (a) Per region observed maximum intensity for the 1979–2009 time period. Regions over the Gulf of Mexico have been removed to test the hypothesis that the MRI-AGCM does not capture the sensitivity of TC maximum intensity to SST because it fails to generate enough TCs over the Gulf of Mexico. Intensity is given in units of m s^{-1}. Per region simulated maximum intensity for the MRI-AGCM is shown in Figure 6b. Note that only those regions with mean August–October SST $\geq$ 25°C are shown.

regardless of whether maximum wind speed or minimum sea level pressure is used as the metric of TC intensity.

It should be noted that to estimate the sensitivity of maximum TC intensity to SST, we use per region mean August–October SST, where SST is temporally averaged over the relevant period (e.g., 1979–2009 for observations and the MRI-AGCM). We also tested as a predictor the per region mean August–October SST from the year during which the per region maximum intensity occurred. In other words, SSTs were not temporally averaged over the entire study period, but were instead matched with the year of the highest TC intensity for each region. Interestingly, the amount of variance in per region maximum intensity described by the nontemporally averaged SSTs does not significantly exceed the variance described by the temporally averaged SSTs. In fact, when we use the per region monthly SST value corresponding to the year *and* month of the per region maximum TC intensity, the amount of variance described by SST decreases. We speculate that this occurs as a result of TC-induced ocean mixing. Strong winds associated with intense TCs mix the upper layer of the ocean, causing cooler subsurface water to move to the surface [*Price*, 1981; *Price et al.*, 2008]. Because it may take several weeks for SSTs to rebound [*Hart et al.*, 2007], if a region experienced a significant amount of TC activity or a particularly intense TC, then this could result in a negative monthly SST anomaly for that region. Because we are primarily interested in the climatological effect of SST on TC intensity and not the reverse relationship, we use the temporally averaged August–October SSTs.

3.2. Quantifying Error Associated With the Spatial Method

The sensitivity of maximum TC intensity to SST obtained in the previous section is estimated based on a certain set of tessellated regions. It is possible that the sensitivity value is partially dependent upon the specific configuration of regions used. For large regions, a slight offset in region boundaries could potentially affect the results. To quantify the error associated with the specific location of the hexagon tessellation, we generate 100 different tessellations using hexagons of the same size but with each tessellation slightly spatially offset. For each tessellation, we estimate the sensitivity of maximum TC intensity to SST for observed and model-generated TCs. An examination of the histograms of sensitivity values obtained using the 100 different tessellations suggests that the spatial method does in fact add error (Figure 8). The sensitivities for observed TCs are all positive and statistically significant, ranging from 3 to 11 m s^{-1}°C^{-1}. Importantly, the only model for which the histograms of observed and modeled sensitivities

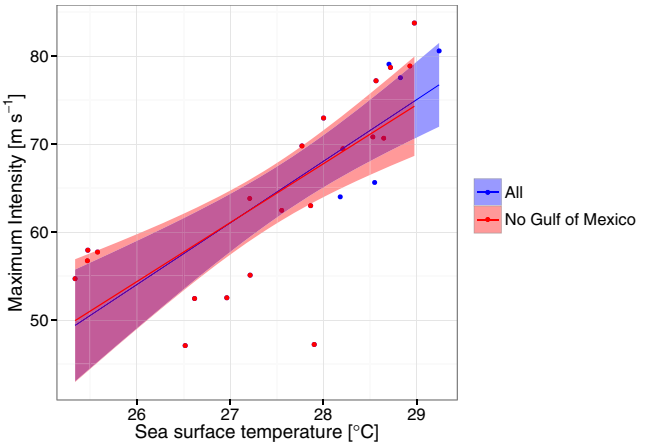

Figure 7. A comparison of the observed sensitivity of per region maximum intensity to SST for all regions (blue) and for regions not covering the Gulf of Mexico, as shown in Figure 6a (red). Observed data from the 1979 to 2009 period are used.

significantly overlap is the CAM5 0.25°. Overall, the distribution of observed sensitivities is flatter than the distributions of simulated sensitivities. Additionally, the sensitivity histograms for model-generated data all include zero. Although this exercise suggests that there is nontrivial error associated with the spatial method applied, it also demonstrates the robustness of the sensitivity results. With the possible exception of the CAM5 0.25°, the sensitivity of observed maximum TC intensity to SST is statistically greater than the sensitivity of simulated maximum TC intensity to SST. Furthermore, the sensitivities are not statistically different from zero for most model-generated TCs.

4. The Sensitivity of TC Potential Intensity to SST: An Intermodel Comparison

Previous results from *Strazzo et al*. [2015] demonstrate that although the relatively lower-resolution FSU-COAPS model does not reproduce the observed sensitivity of TC maximum intensity to SST, it successfully captures the sensitivity of TC potential intensity to SST. *Strazzo et al*. [2015] speculate that insufficient resolution was to blame. However, we have seen so far that even relatively high-resolution models do not capture the sensitivity of TC intensity to SST. Next we examine whether these models, like the FSU-COAPS, capture the sensitivity of potential intensity to SST. To test this, we find the per region maximum potential intensity, where potential intensity is calculated from reanalysis and model gridded data using Kerry Emanuel's algorithm (available from ftp://texmex.mit.edu/pub/emanuel/TCMAX/), translated to the R language by Thomas Jagger.

Overall, the spatial patterns of simulated potential intensity match the spatial pattern of observed potential intensity, where observed potential intensity refers to values obtained using reanalysis atmospheric fields (Figure 9). When we examine the per region difference in observed and simulated potential intensity, we find that the differences are not consistent among the models (Figure 10). For example, the MRI-AGCM tends to underestimate potential intensity while the remaining models tend to overestimate potential intensity. The FSU-COAPS model overestimates potential intensity by as much as 9.69 m s^{-1} while the MRI-AGCM underestimates potential intensity by as much as 4.15 m s^{-1}. Despite these differences in per region values, the simulated patterns of potential intensity better match the observed pattern.

Table 3. Summaries of Regressions of Per Region Minimum Sea Level Pressure onto Average August–October SST for Observations and GCMs[a]

Data Set	Sensitivity	95% C.I.
Observations	−14	(−19.2, −8.85)
MRI-AGCM	1.4	(−4.98, 7.82)
CAM5 0.25°	−1.3	(−7.14, 4.62)
GFDL-HiRAM	0.95	(−4.16, 6.05)
FSU-COAPS	5.7	(−0.837, 12.3)
CAM5 1°	4.3	(−1.51, 10.04)

[a]The second column provides the sensitivity of minimum sea level pressure to SST while the third column provides the 95% confidence interval (C.I.) on this estimate. Sensitivity estimates have units of hPa/°C warming. For each model, the per region minimum sea level pressure intensity represents the minimum sea level pressure for each region over the simulation time periods given in Table 1. Additionally, only those regions with mean August–October SST $\geq$ 25°C are used in the regressions.

Next we calculate the sensitivity of potential intensity to SST by regressing the set of per region maximum potential intensities onto the set of per region mean August–October SSTs (Figure 11). For a more direct comparison with the sensitivity of maximum intensity to SST, we calculate the sensitivity of potential intensity to SST using only those regions with mean August–October SST of at least 25°C. As demonstrated in *Strazzo et al*. [2015], the observed sensitivity of maximum intensity to SST nearly matches the observed sensitivity of potential intensity to SST. In other words, the most intense

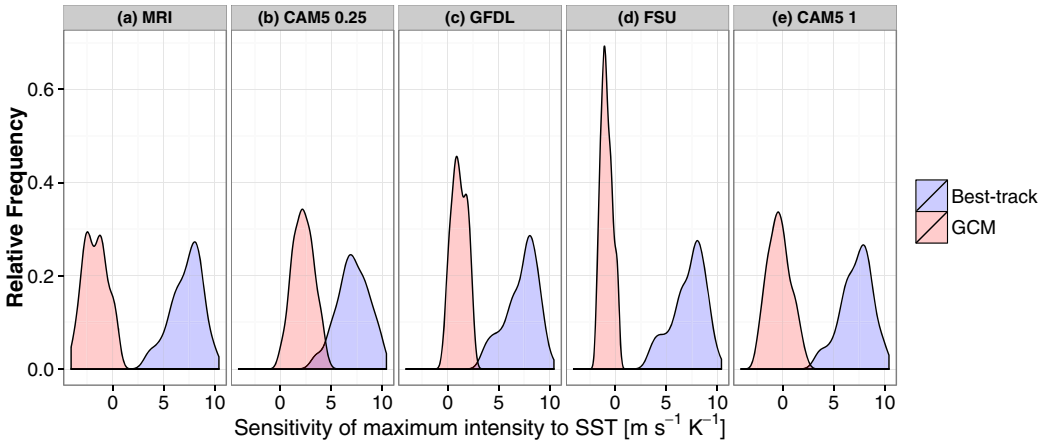

Figure 8. Density plots of sensitivity values obtained using 100 different hexagon tessellations, each slightly offset spatially from the others. The regions remain the same size, but the specific origin location of the tessellation changes. For each tessellation, the sensitivity of observed and modeled maximum TC intensity to SST is calculated. The range of sensitivity values represents error associated with the spatial tessellation method. Error is estimated for observations and the (a) MRI-AGCM, (b) CAM5 0.25°, (c) GFDL-HiRAM, (d) FSU-COAPS, and (e) CAM5 1°. Red shading indicates model sensitivity values while blue shading represents observed sensitivity values calculated for the respective model period. Note that observed sensitivities in Figure 8e were calculated using all hexagons, even those with fewer than 15 TCs, for a more direct comparison with the CAM5 1°.

observed TCs form where we might expect on the basis of potential intensity theory. Interestingly, all of the models reproduce the observed sensitivity of potential intensity to SST relatively well (Table 4). Even the MRI-AGCM, which generally underestimates potential intensity (Figure 10), manages to capture the sensitivity of potential intensity to SST. Regardless of horizontal resolution, the models generate the environment necessary for the formation of strong TCs over the correct portions of the basin. Despite this, strong simulated TCs either do not form (CAM5 1°, FSU-COAPS, and GFDL-HiRAM) or do not form where we might expect them to form on the basis of potential intensity theory (MRI-AGCM and to a lesser degree, CAM5 0.25°). Although the higher-resolution climate models yield more category 4 and 5 TCs, we find that the strongest of these storms do not necessarily form over regions with high simulated potential intensity—regions where the climatological thermodynamic conditions support the formation of strong TCs. This contrasts with observed TCs, which are generally most intense over regions with the highest potential intensity.

Although the explanation for this discrepancy is not certain, it may be a result of model parameterizations that do not adequately represent TC inner core physics. This explanation would support the idea that model resolution on the order of 1 km is required to resolve TC convection and core physics [*Chen et al.*, 2007]. The discrepancy between observed and simulated sensitivity also may be explained by errors in simulated environmental conditions (e.g., vertical wind shear, vorticity) that are thought to influence TC intensity [*DeMaria*, 1996; *Wong and Chan*, 2004]. Indeed, we find that the CAM5 1°, the FSU-COAPS, and the MRI GCMs all tend to simulate higher August–October mean vertical wind shear over the Gulf of Mexico than is present in the MERRA data (Figure 12). It is possible that deficiencies in dynamical model fields play a role in inhibiting TC intensity over the Gulf of Mexico, although it should be noted that FSU-COAPS climatological vertical wind shear is actually higher over regions with the highest simulated maximum intensities.

Interestingly, none of the GCM simulations yield a statistically significant relationship between per region maximum intensity and vertical wind shear. Conversely, per region observed maximum intensity decreases by 1.5 ± 0.556 m s^{-1} for every 1 m s^{-1} increase in vertical wind shear. Although the models fail to reproduce the sensitivity of TC intensity to wind shear, they successfully capture the strong negative correlation between wind shear and SST. Regions with the warmest SSTs also are on average those regions with the lowest observed and simulated wind shear values. Research by *Kossin and Vimont* [2007] and *Vimont and Kossin* [2007] suggests that these covarying relationships among SST and other environmental variables (e.g., wind shear, relative humidity, static stability) modulate North Atlantic TC activity. Despite capturing the observed correlation between wind shear and SST, the models still fail to simulate stronger TCs in those environments that are more favorable (at least in terms of shear and SST) for intense TCs. Additional

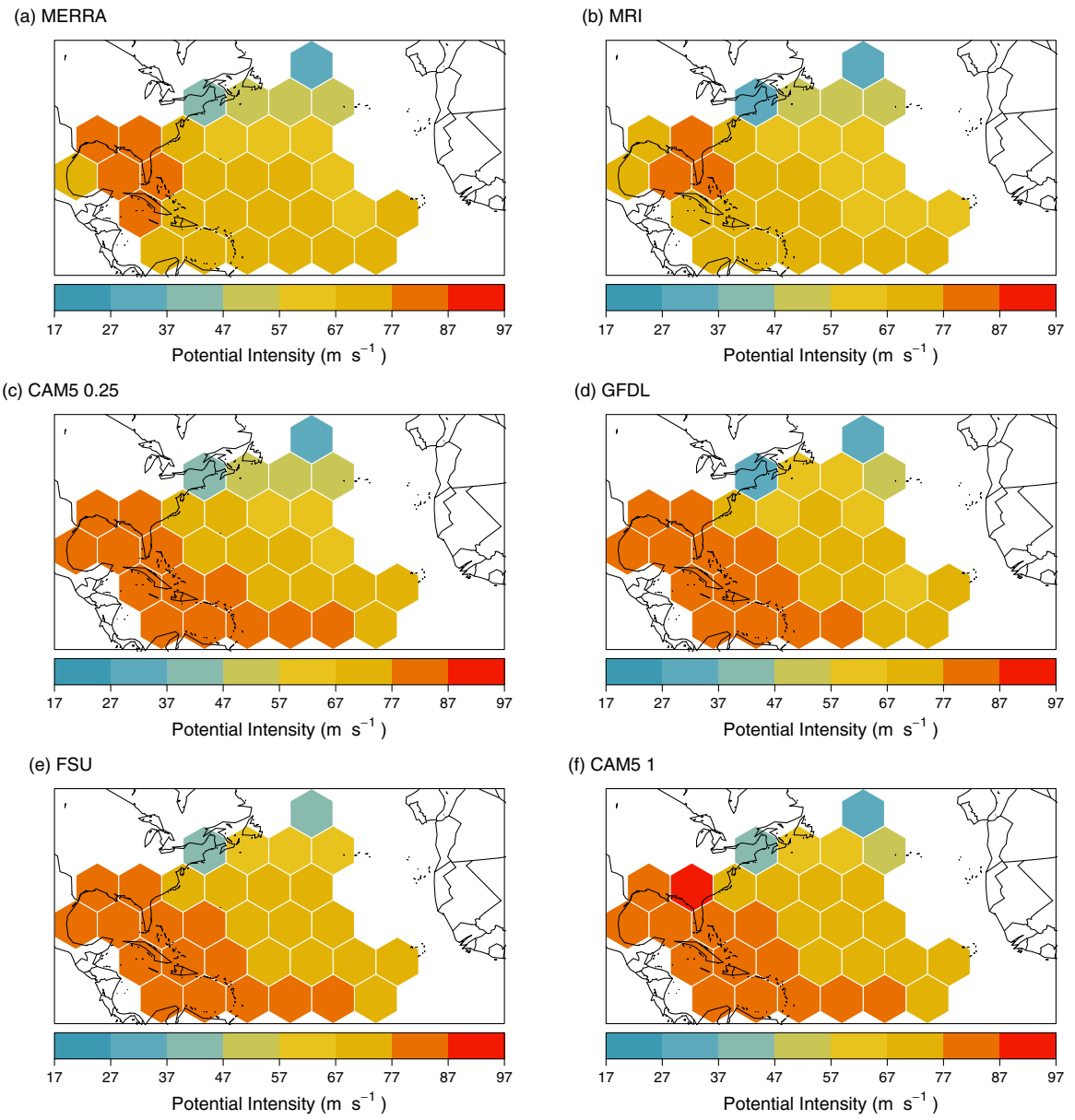

Figure 9. The per region maximum potential intensity (m s^{-1}) calculated from (a) MERRA, (b) MRI-AGCM, (c) CAM5 0.25°, (d) GFDL-HiRAM, (e) FSU-COAPS, and (f) CAM5 1° models.

research is needed to address whether GCMs successfully capture the observed covariance of other relevant environmental fields.

5. Summary and Discussion

Previous research demonstrated the inability of two climate models to capture the observed sensitivity of maximum TC intensity to SST; however, it remained unclear whether higher model resolution would improve the simulated sensitivity. Given this need to better understand the influence of resolution on the ability of GCMs to simulate the physically relevant relationship between maximum TC intensity and SST, we expand upon previous research by examining the sensitivity for two higher-resolution GCMs and one additional lower-resolution GCM. In addition to the 50 km resolution GFDL-HiRAM and 0.94° resolution FSU-COAPS models, we estimate the sensitivity of maximum TC intensity to SST for model-generated TCs from the 0.25° CAM5, the 20 km MRI-AGCM, and the 1° CAM5. Results suggest that while increasing model resolution does permit the development

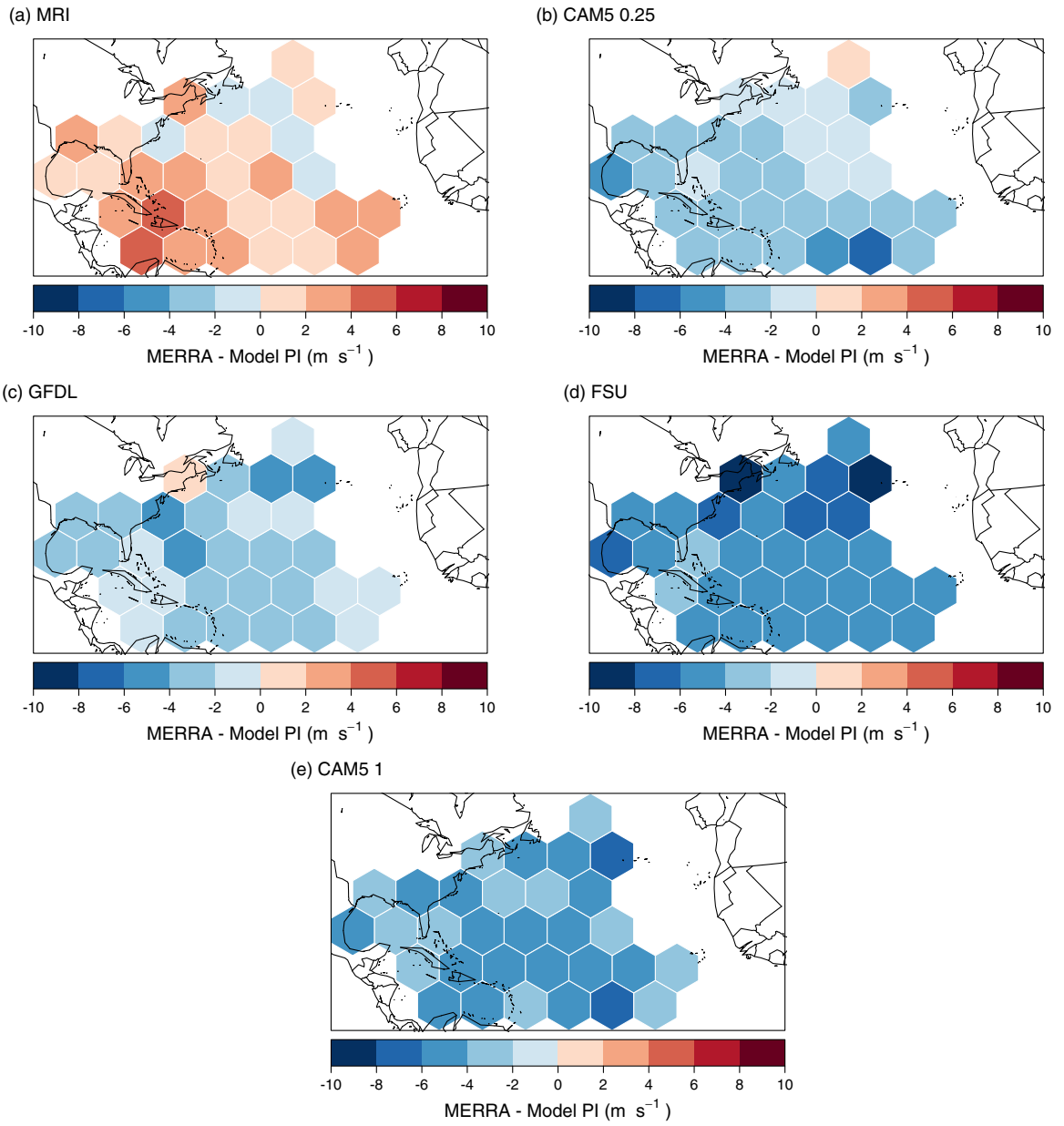

Figure 10. Difference maps depicting the difference in observed (MERRA)—simulated (model) per region maximum potential intensity (PI) in units of m s^{-1} for the (a) MRI-AGCM, (b) CAM5 0.25°, (c) GFDL-HiRAM, (d) FSU-COAPS, and (e) CAM5 1° models.

of higher intensity model-generated TCs, the statistical relationship between simulated maximum TC intensity and SST does not necessarily improve. For example, the highest-resolution model considered here—the MRI-AGCM—does not reproduce the observed sensitivity of maximum intensity to SST. Although neither the CAM5 0.25° nor the MRI-AGCM yield statistically significant sensitivity values at the 95% confidence level, the sensitivity values for the CAM5 0.25° are significant at the 90% confidence level. Because both versions of the CAM5 have essentially the same large-scale monthly climatology and use the same parameterization schemes, the increased sensitivity of the CAM5 0.25° compared to the CAM5 1° is likely due to improved resolution. Therefore, there is reason to be hopeful that improving model resolution may yield more realistic simulated TCs, even for models that parameterize many of the processes associated with TC intensification.

An examination of the spatial distributions of simulated TC activity reveals that the models are unable to reproduce the observed spatial pattern of TCs. Importantly, the MRI-AGCM, GFDL-HiRAM, and FSU-COAPS

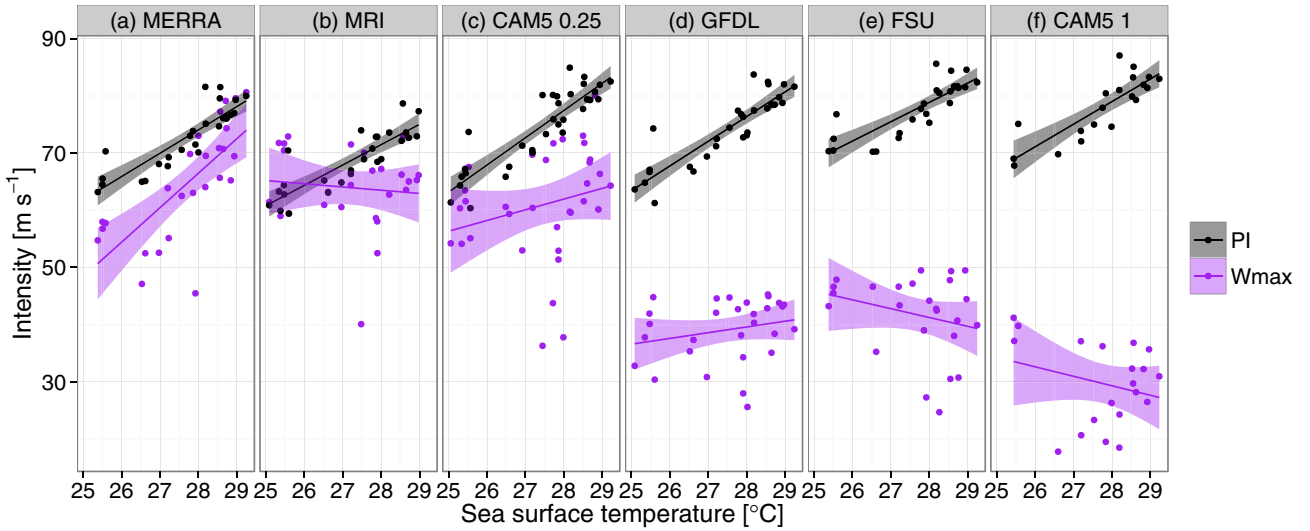

Figure 11. Regressions of regional maximum potential intensity onto regional mean August–October SST for reanalysis (a) MERRA, (b) the MRI-AGCM, (c) CAM5 0.25°, (d) GFDL-HiRAM, (e) FSU-COAPS, and (f) CAM5 1° models. The sensitivities of maximum TC intensity to SST are given by the slope of the purple lines while the black lines represent the sensitivity of maximum potential intensity to SST. The shading represents the 95% confidence interval about the regression. Maximum and maximum potential intensity are shown in units of m s^{-1} and SST is shown in units of °C. For each regression, only regions with at least 15 TCs are used, with the exception of the CAM5 1°, which generated too few TCs to apply this rule. Additionally, only those regions with mean August–October SST $\geq$ 25°C are used in the regressions.

models do not generate or track as many TCs over the Gulf of Mexico as are observed during the same time period. Additionally, simulated TCs that do form or move over this region tend to be relatively weak. What is not entirely clear from these results is whether the lack of TCs over this region is caused by model errors in larger scale features or imperfect parameterization of shallow/deep convection. Results presented in *Strazzo et al.* [2015] suggest that model errors in larger scale features are partially to blame. *Manganello et al.* [2012] attribute the inability of the ECMWF integrated forecast system to capture the observed spatial distribution of TC activity to model errors in the large-scale environmental conditions. Furthermore, they show that these errors tend to be fairly consistent regardless of the resolution used for the model run. However, we find that the observed sensitivity of TC maximum intensity to SST for only those regions outside of the Gulf of Mexico is not statistically different from the observed sensitivity calculated using *all* regions. This suggests that while model errors associated with large-scale atmospheric features may be important for determining whether model-generated TCs track over the Gulf of Mexico, these errors do not fully explain the inability of GCMs to capture the sensitivity of observed TC intensity to SST.

Table 4. Summaries of Regressions of Per Region Potential Intensity onto Average August–October SST for Observations (MERRA) and GCMs[a]

Data Set	Sensitivity	95% C.I.
MERRA (obs)	4.1	(3.10, 5.05)
MRI-AGCM	3.6	(2.64, 4.46)
CAM5 0.25°	4.8	(3.85, 5.67)
GFDL-HiRAM	4.3	(3.42, 5.21)
FSU-COAPS	3.4	(2.41, 4.34)
CAM5 1°	3.9	(2.67, 4.22)

[a]The second column provides the sensitivity of potential intensity to SST while the third column provides the 95% confidence interval (C.I.) on this estimate. Sensitivity estimates have units of m s^{-1}/°C warming. For each model, the per region maximum potential intensity represents the highest potential intensity for each region over the simulation time periods given in Table 1. Additionally, only those regions with mean August–October SST $\geq$ 25°C are used in the regressions.

We also estimate error associated with the spatial tessellation method to better understand the statistical significance of our results. We find that the specific location of the hexagon tessellation impacts the sensitivity of per region maximum intensity to SST. Observed sensitivities range from 3 to 11 m s^{-1}°C^{-1}, while the simulated sensitivities include zero for every model. This supports the conclusion that observed maximum TC intensity is significantly sensitive to SST while modeled maximum TC intensity is not. Note that error associated with region size is not addressed here. Small changes to the region size likely have a similar effect on the sensitivity as shifts in the tessellation location. We are limited in how much region size may be altered as we must balance (a) having sufficient TC data per region, and (b) having enough regions with which to generate a regression.

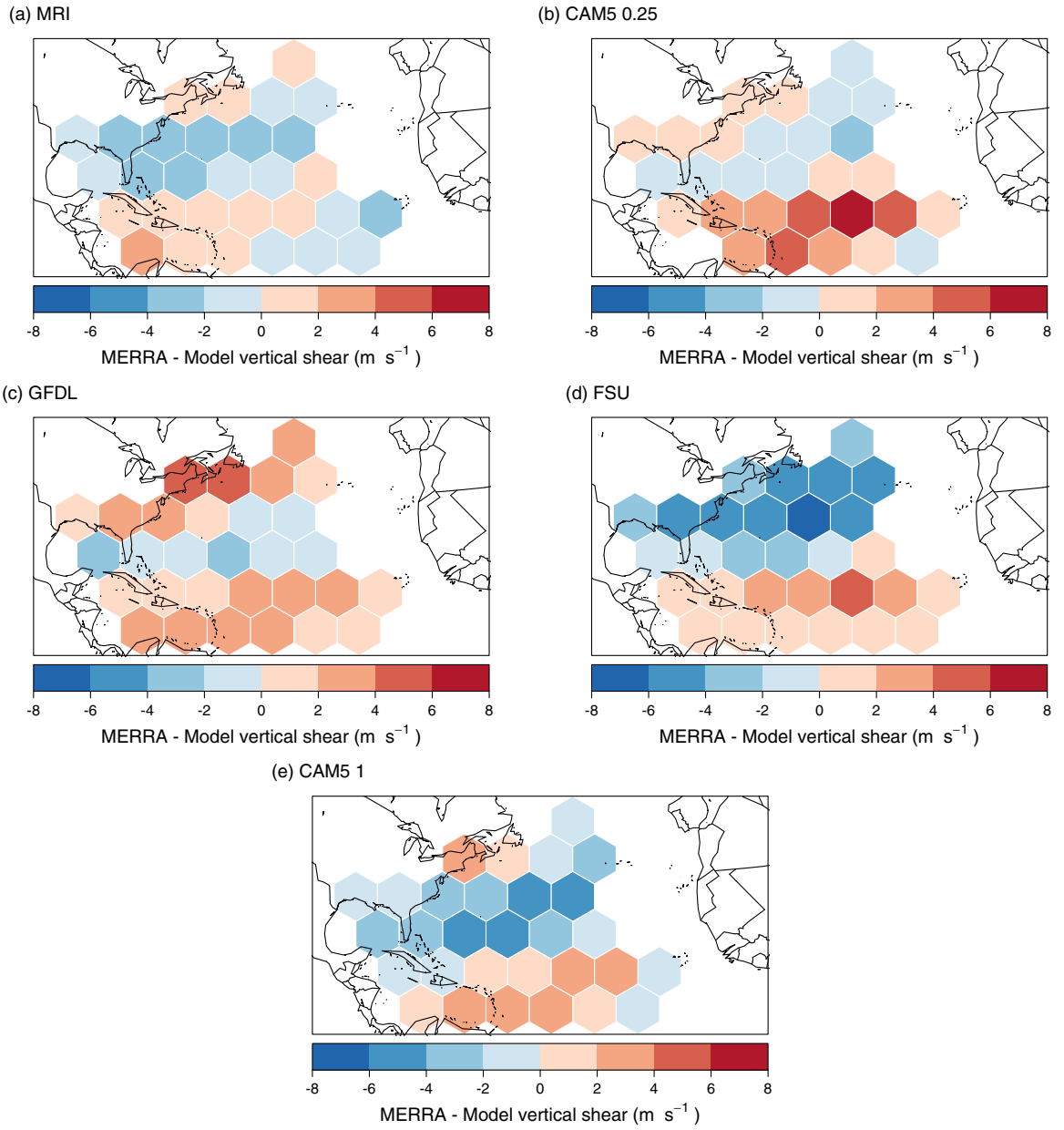

Figure 12. Difference maps depicting per region mean August–October reanalyzed (MERRA)—simulated 850–200 hPa vertical wind shear for each of the models.

Finally, we expand upon the results presented in *Strazzo et al.* [2015] and compare the sensitivity of observed and simulated potential intensity for all five model configurations at our disposal. Results indicate the models reproduce the observed spatial pattern and sensitivity of per region maximum potential intensity to SST very well. Regions with high observed and simulated potential intensity correspond to regions with high mean August–October SST. The most intense observed TCs tend to form over regions with the highest potential intensity. Conversely, we find that the most intense simulated TCs do not necessarily form over regions with the highest simulated potential intensity, regardless of model resolution. We show that the FSU-COAPS model over-predicts vertical wind shear over the portions of the basin with the highest observed intensities, which may influence the frequency and intensity of simulated TCs over this region. Therefore, it is possible that the discrepancy between simulated maximum TC intensity and potential intensity results from model errors in the relevant atmospheric fields. On the other hand, the explanation may be related to the inability of GCMs to capture TC inner core thermodynamic processes.

These results demonstrate that even if a model is capable of resolving TCs with intensities exceeding 68 m s^{-1}, and even if the model reasonably simulates potential intensity, it may not necessarily capture the sensitivity of maximum intensity to SST. There are numerous factors that may influence this sensitivity. For example, several studies investigate the influence of the parameterization scheme on simulated TC activity [e.g., *Knutson and Tuleya*, 2004; *Reed and Jablonowski*, 2011; *Kim et al*., 2012; *Zhao et al*., 2012; *Lim et al*., 2015]. As noted previously, besides the two versions of the CAM5, each of the models we examine utilizes different convective parameterizations, which may affect the simulation results. Additionally, the algorithms used to detect and track TCs in the model fields vary among the models. As demonstrated in *Horn et al*. [2014], model simulation results are often sensitive to differences in the duration threshold, which ranges from 36 to 72 h for the models used in this study. It is possible that we filtered out this tracker effect by considering only the strongest TCs (i.e., those that are most likely to be detected regardless of the selected tracking algorithm). Regardless, future research is necessary to identify which of these factors most strongly influences a climate model's ability to capture the sensitivity of maximum TC intensity to SST.

Acknowledgments

We are grateful for the constructive feedback Jim Kossin and two anonymous reviewers provided during the review of this paper. We also thank Baoqiang Xiang for comments and suggestions provided during a NOAA internal review. JBE was supported by a grant from the Risk Prediction Initiative (RPI) of the Bermuda Institute of Ocean Sciences (BIOS). HM was supported by the program "Projection of the Change in Future Weather Extremes Using Super-High-Resolution Atmospheric Models" funded by the KAKUSHIN and SOUSEI programs of the Ministry of Education, Culture, Sports, Science, and Technology (MEXT) of Japan. Calculations by the MRI-AGCM3.2 were performed on the Earth Simulator. TEL received grant support from the U.S. Department of Energy Office of Science and the NOAA Climate Program Office. MW was supported by the Regional and Global Climate Modeling Program of the Office of Biological and Environmental Research in the Department of Energy Office of Science under contract DE-AC02-05CH11231. Observed tropical cyclone data used in this paper were obtained from http://www.nhc.noaa.gov/data/#hurdat, and the code used to interpolate the TC data can be found at http://www.hurricaneclimate.com/. SST data were downloaded from http://www.metoffice.gov.uk/hadobs/hadisst/data/download.html, and MERRA reanalysis data were downloaded from http://disc.sci.gsfc.nasa.gov/mdisc/data-holdings/merra/merra_products_nonjs.shtml. Simulated TC track data are available upon request. The code used to generate these results is available at http://rpubs.com/sestrazz/modelRes.

References

Bister, M., and K. A. Emanuel (1998), Dissipative heating and hurricane intensity, *Meteorol. Atmos. Phys.*, *65*(3–4), 233–240.

Bretherton, C. S., J. R. McCaa, and H. Grenier (2004), A new parameterization for shallow cumulus convection and its application to marine subtropical cloud-topped boundary layers. Part I: Description and 1D results, *Mon. Weather Rev.*, *132*(4), 864–882.

Camargo, S. J. (2013), Global and regional aspects of tropical cyclone activity in the CMIP5 models, *J. Clim.*, *26*(24), 9880–9902.

Camargo, S. J., A. G. Barnston, and S. E. Zebiak (2005), A statistical assessment of tropical cyclone activity in atmospheric general circulation models, *Tellus, Ser. A*, *57*, 589–604.

Caron, L. P., C. G. Jones, and K. Winger (2011), Impact of resolution and downscaling technique in simulating recent Atlantic tropical cyclone activity, *Clim. Dyn.*, *37*(5–6), 869–892.

Chen, S. S., W. Zhao, M. A. Donelan, J. F. Price, and E. J. Walsh (2007), The CBLAST-Hurricane program and the next-generation fully coupled atmosphere-wave-ocean models for hurricane research and prediction, *Bull. Am. Meteorol. Soc.*, *88*, 311–317.

Christensen, J. H., K. Krishna Kumar, E. Aldrian, S.-I. An, I. F. A. Cavalcanti, M. de Castro, W. Dong, P. Goswami, A. Hall, J. K. Kanyanga, et al., (2013), *Climate phenomena and their relevance for future regional climate change. In Climate Change 2013: The Physical Science Basis. Contribution of Working Group I to the Fifth Assessment Report of the Intergovernmental Panel on Climate Change*, edited by T. F. Stocker, et al., pp. 1248–1251, Cambridge Univ. Press, Cambridge, U. K.

DeMaria, M. (1996), The effect of vertical shear on tropical cyclone intensity change, *J. Atmos. Sci.*, *53*(14), 2076–2087.

DeMaria, M., and J. Kaplan (1994), Sea surface temperature and the maximum intensity of Atlantic tropical cyclones. *J. Clim.*, *7*(9), 1324–1334.

Elsner, J. B., and T. H. Jagger (2013), *Hurricane Climatology: A Modern Statistical Guide Using R*, Oxford Univ. Press, N. Y.

Elsner, J. B., J. P. Kossin, and T. H. Jagger (2008), The increasing intensity of the strongest tropical cyclones. *Nature*, *455*(7209), 92–95.

Elsner, J. B., R. E. Hodges, and T. H. Jagger (2012a), Spatial grids for hurricane climate research, *Clim. Dyn.*, *39*, 21–36.

Elsner, J. B., J. C. Trepanier, S. E. Strazzo, and T. H. Jagger (2012b), Sensitivity of limiting hurricane intensity to ocean warmth, *Geophys. Res. Lett.*, *39*, L17702, doi:10.1029/2012GL053002.

Elsner, J. B., S. E. Strazzo, T. H. Jagger, T. E. LaRow, and M. Zhao (2013), Sensitivity of limiting hurricane intensity to SST in the Atlantic from observations and GCMs, *J. Clim.*, *26*(16), 5949–5957.

Emanuel, K. A. (1986), An air-sea interaction theory for tropical cyclones. Part I: Steady-state maintenance. *J. Atmos. Sci.*, *43*(6), 585–605.

Hart, R. E., R. N. Maue, and M. C. Watson (2007), Estimating local memory of tropical cyclones through MPI anomaly evolution, *Mon. Weather Rev*, *135*(12), 3990–4005.

Hogan, T. F., and T. E. Rosmond (1991), The description of the Navy Operational Global Atmospheric Prediction System's spectral forecast model, *Mon. Weather Rev.*, *119*(8), 1786–1815.

Horn, M., et al. (2014), Tracking scheme dependence of simulated tropical cyclone response to idealized climate simulations, *J. Clim.*, *27*(24), 9197–2913.

Kim, D., A. H. Sobel, A. D. Del Genio, Y. Chen, S. J. Camargo, M. S. Yao, M. Kelley, and L. Nazarenko (2012), The tropical subseasonal variability simulated in the NASA GISS general circulation model, *J. Clim.*, *25*(13), 4641–4659.

Kim, H. S., G. A. Vecchi, T. R. Knutson, W. G. Anderson, T. L. Delworth, A. Rosati, F. Zeng, and M. Zhao (2014), Tropical cyclone simulation and response to CO_2 doubling in the GFDL CM2. 5 high-resolution coupled climate model, *J. Clim.*, *27*(21), 8034–8054.

Knutson, T. R., and R. E. Tuleya (2004), Impact of CO_2-induced warming on simulated hurricane intensity and precipitation: Sensitivity to the choice of climate model and convective parameterization, *J. Clim.*, *17*, 3477–3495.

Knutson, T. R., J. J. Sirutis, S. T. Garner, I. M. Held, and R. E. Tuleya (2007), Simulation of the recent multidecadal increase of Atlantic hurricane activity using an 18-km-grid regional model, *Bull. Am. Meteorol. Soc.*, *88*(10), 1549–1565.

Knutson, T. R., J. L. McBride, J. Chan, K. Emanuel, G. Holland, C. Landsea, I. Held, J. P. Kossin, A. K. Srivastava, and M. Sugi (2010), Tropical cyclones and climate change, *Nat. Geosci.*, *3*, 157–163.

Kossin, J. P. (2014), Validating atmospheric reanalysis data using tropical cyclones as thermometers, *Bull. Am. Meteorol. Soc.*, *96*, 1089–1096.

Kossin, J. P., and D. J. Vimont (2007), A more general framework for understanding Atlantic hurricane variability and trendss, *Bull. Am. Meteorol. Soc.*, *88*, 1767–1781.

Landsea, C. W., and J. L. Franklin (2013), Atlantic hurricane database uncertainty and presentation of a new database format. *Mon. Weather Rev.*, *141*(10), 3576–3592.

LaRow, T. E., Y. K. Lim, D. W. Shin, E. P. Chassignet, and S. Cocke (2008), Atlantic basin seasonal hurricane simulations, *J. Clim.*, *21*, 3191–3206.

Lim, Y. K., S. D. Schubert, O. Reale, M. I. Lee, A. M. Molod, and M. J. Suarez (2015), Sensitivity of tropical cyclones to parameterized convection in the NASA GEOS5 model, *J. Clim.*, *28*(2), 551–573.

Manganello, J. V., et al. (2012), Tropical cyclone climatology in a 10-km global atmospheric GCM: Toward weather-resolving climate modeling, *J. Clim.*, *25*(11), 3867–3893.

Mizuta, R., et al. (2012), Climate simulations using MRI-AGCM3.2 with 20-km grid, *J. Meteorol. Soc. Jpn.*, *90A*, 233–258.
Murakami, H., and M. Sugi (2010), Effect of model resolution on tropical cyclone climate projections, *Sola*, *6*, 73–76.
Murakami, H., B. Wang, and A. Kitoh (2011), Future change of Western North Pacific Typhoons: Projections by a 20-km-mesh global atmospheric model, *J. Clim.*, *24*(4), 1154–1169.
Murakami, H., et al. (2012), Future changes in tropical cyclone activity projected by the new high-resolution MRI-AGCM, *J. Clim.*, *25*(9), 3237–3260.
Park, S., and C. S. Bretherton (2009), The University of Washington shallow convection and moist turbulence schemes and their impact on climate simulations with the Community Atmosphere Model, *J. Clim.*, *22*(12), 3449–3469.
Price, J. F. (1981), Upper ocean response to a hurricane, *J. Phys. Oceanogr.*, *11*(2), 153–175.
Price, J. F., J. Morzel, and P. P. Niiler (2008), Warming of SST in the cool wake of a moving hurricane, *J. Geophys. Res.*, *113*, C07010, doi: 10.1029/2007JC004393.
Reed, K. A., and C. Jablonowski (2011), Impact of physical parameterizations on idealized tropical cyclones in the Community Atmosphere Model, *Geophys. Res. Lett.*, *38*, L04805, doi:10.1029/2010GL046297.
Rayner, N. A., D. E. Parker, E. B. Horton, C. K. Folland, L. V. Alexander, D. P. Powell, E. C. Kent, and A. Kaplan (2003), Global analyses of sea surface temperature, sea ice, and night marine air temperature since the late nineteenth century, *J. Geophys. Res.*, *108*(D14), 4407, doi: 10.1029/2002JD002670.
Rienecker, M. V., et al. (2011), MERRA: NASA's modern-era retrospective analysis for research and applications, *J. Clim.*, *24*(14), 3624–3648.
Roberts, M. J., P. L. Vidale, M. S. Mizielinski, M. E. Demory, R. Schiemann, J. Strachan, K. Hodges, R. Bell, and J. Camp, (2015), Tropical cyclones in the UPSCALE ensemble of high resolution global climate models, *J. Clim.*, *28*(2), 574–596.
Strachan, J., P. L. Vidale, K. Hodges, M. Roberts, and M. E. Demory (2013), Investigating global tropical cyclone activity with a hierarchy of AGCMs: The role of model resolution, *J. Clim.*, *26*(1), 133–152.
Strazzo, S., J. B. Elsner, T. LaRow, D. J. Halperin, and M. Zhao (2013a), Observed versus GCM-generated local tropical cyclone frequency: Comparisons using a spatial lattice, *J. Clim.*, *26*(21), 8257–8268.
Strazzo, S., J. B. Elsner, J. C. Trepanier, and K. A. Emanuel (2013b), Frequency, intensity, and sensitivity to sea surface temperature of North Atlantic tropical cyclones in best-track and simulated data, *J. Adv. Model. Earth Syst.*, *5*, 500–509, doi:10.1002/jame.20036.
Strazzo, S. E., J. B. Elsner, and T. E. LaRow (2015), Quantifying the sensitivity of maximum, limiting, and potential tropical cyclone intensity to SST: Observations versus the FSU/COAPS global climate model, *J. Adv. Model. Earth Syst.*, *7*, 586–599, doi:10.1002/2015MS000432.
Tiedtke, M. (1989), A comprehensive mass flux scheme for cumulus parameterization in large-scale models. *Mon. Weather Rev.*, *117*(8), 1779–1800.
Vecchi, G. A., S. Fueglistaler, I. M. Held, T. R. Knutson, and M. Zhao (2013), Impacts of atmospheric temperature trends on tropical cyclone activity, *J. Clim.*, *26*(11), 3877–3891.
Villarini, G., G. A. Vecchi, T. R. Knutson, M. Zhao, and J. A. Smith (2011), North Atlantic tropical storm frequency response to anthropogenic forcing: Projections and sources of uncertainty, *J. Clim.*, *24*(13), 3224–3238.
Vimont, D. J., and J. P. Kossin (2007), The Atlantic meridional mode and hurricane activity, *Geophys. Res. Lett.*, *34*, L07709, doi:10.1029/2007GL029683.
Walsh, K., S. Lavender, E. Scoccimarro, and H. Murakami (2013), Resolution dependence of tropical cyclone formation in CMIP3 and finer resolution models, *Clim. Dyn.*, *40*(3–4), 585–599.
Walsh, K. J. E., S. J. Camargo, G. A. Vecchi, A. S. Daloz, J. Elsner, K. Emanuel, M. Horn, Y. K. Lim, M. Roberts, C. Patricola, et al. (2015), Hurricanes and climate: The US CLIVAR working group on hurricanes, *Bull. Amer. Meteorol. Soc.*, *96*, 997–1017.
Wehner, M. F., et al. (2014), The effect of horizontal resolution on simulation quality in the Community Atmospheric Model, CAM5.1, *J. Adv. Model. Earth Syst.*, *6*, 980–997, doi:10.1002/2013MS000276.
Wehner, M. F., K. A. Reed, D. Stone, W. D. Collins, and J. Bacmeister (2015), Resolution dependence of future tropical cyclone projections of CAM5.1 in the US CLIVAR Hurricane Working Group idealized configurations, *J. Clim.*, *28*(10), 3905–3925.
Wong, M. L. M., and J. C. L. Chan (2004), Tropical cyclone intensity in vertical wind shear, *J. Atmos. Sci.*, *61*(15), 1859–1876.
Yoshimura, J., and M. Sugi (2005), Tropical cyclone climatology in a high-resolution AGCM-Impacts of SST warming and CO2 increase, *Sola*, *1*, 133–136.
Yoshimura, J., R. Mizuta, and H. Murakami (2015), A spectral cumulus parameterization scheme interpolating between two convective updrafts with semi-Lagrangian calculation of transport by compensatory subsidence, *Mon. Weather Rev.*, *143*, 597–621.
Zarzycki, C. M., and C. Jablonowski (2014), A multidecadal simulation of Atlantic tropical cyclones using a variable-resolution global atmospheric general circulation model, *J. Adv. Model. Earth Syst.*, *6*, 805–828, doi:10.1002/2014MS000352.
Zhang, G. J., and N. A. McFarlane (1995), Sensitivity of climate simulations to the parameterization of cumulus convection in the Canadian Climate Centre general circulation model, *Atmos. Ocean*, *33*(3), 407–446.
Zhao, M., I. M. Held, S. J. Lin, and G. A. Vecchi (2009), Simulations of global hurricane climatology, interannual variability, and response to global warming using a 50-km resolution GCM, *J. Clim.*, *22*(24), 6653–6678.
Zhao, M., I. M. Held, S. J. Lin, and G. A. Vecchi (2012), Some counterintuitive dependencies of tropical cyclone frequency on parameters in a GCM, *J. Atmos. Sci.*, *69*, 2272–2283.